Co-Adsorption of Copper(II) and 3-Amino-1,2,4-triazole at a Water–Natural Macromolecular Compound Interface: Molecular Structure from Adsorption Isotherms Combined with X-ray Absorption Measurements

Karine Flogeac,[a] Emmanuel Guillon,*[a] and Michel Aplincourt[a]

Keywords: Adsorption / Environmental chemistry / Pesticides / Structure elucidation / Surface chemistry / X-ray absorption spectroscopy

The co-adsorption of Cu^{II} and amitrole at a water–natural macromolecular compound interface was studied by means of batch adsorption experiments, Fourier transform infrared, and X-ray absorption spectroscopy. The binary systems, aqueous amitrole–Cu^{II} complex, and amitrole and Cu^{II} adsorbed on the surface of the solid were studied. The ternary system was investigated over the pH range 2–10 and at varying metal concentrations. The combination of macroscopic and molecular information shows that Cu^{II} and amitrole interact directly at the water–solid interface to form ternary surface complexes. A two-step mechanism is proposed whereby initial formation of a Cu^{II}–amitrole aqueous complex is followed by the sorption of this complex onto the surface. The structure of the ternary complex was elucidated. Copper(II) is bound to the surface in an inner-sphere mode, while two amitrole ligands simultaneously bonded in a monodentate fashion to Cu^{II} to form a six-membered coordination sphere around the metal cation. The copper coordination sphere is completed by two water molecules. This structure and the mechanism proposed are supported by a combination of potentiometric data, IR and UV/visible spectroscopies and XAS measurements.

Introduction

The monitoring and control of pollutants in the aquatic environment is becoming of increasing concern. Detailed investigations of the interactions between both naturally occurring and anthropogenic species found in the environment have provided information regarding their chemical structure and speciation, and thus the transport, bio-availability and potential toxicity of pollutants.[1–3] In order to fully understand the chemical processes that occur in groundwater, soils and surface waters, it is important to study the role of the solid–water interface as well as the interactions in the aqueous phase. With this aim in mind, this paper investigates ternary surface complexes formed during the adsorption of copper(II) and an organic ligand, 3-amino-1,2,4-triazole (amitrole), onto soil organic matter (SOM). Indeed, there is a lack of mechanistic molecular-level understanding due to the limited knowledge of the speciation and the reactivity of amitrole at the solid–water interface. In this respect, fundamental studies of a simplified model system play an important role since they can provide detailed information about the composition, structure and reactivity of amitrole surface species formed. This information then forms the basis of molecular-level interpretations of observations made on real soils.

It is now widely accepted that SOM, and notably lignin materials, plays a key role in the regulation of metal ions and other pollutants in the environment.[4–7] Lignin is a natural polymer that is produced biologically by random polymerisation processes, which make its study complicated.[8] It is a cross-linked, phenolic polymer built from three basic phenyl propane monomers (*p*-hydroxycinnamyl, coniferyl, and sinapyl alcohols), which are responsible for its chemical heterogeneity. Thus, the solid studied as a model for SOM is a lignocellulosic substrate (LS) extracted from wheat straw by acid/base treatments.

Amitrole is a herbicide that is widely used all over the world. It is used as a systematic herbicide for total weed control in vineyards, orchards, forests, non-crop areas and in aquatic environments such as marshes and drainage ditches.[9] Amitrole is quickly absorbed through the leaves and then migrates into plant tissues to inhibit several biochemical pathways. Moreover, it is often associated with other well-known herbicides such as glyphosate or paraquat. Several studies have been devoted to the adsorption of amitrole in soils but they were essentially focused on quantitative aspects.[10–15] The primary objective of this work is to identify the molecular mechanism(s) of Cu^{II}–amitrole coadsorption on LS. We present new data for the ternary Cu^{II}/amitrole/LS system. Conclusions are drawn based on a comparison of new XAS spectroscopic data and quantita-

[a] GRECI (Groupe de Recherche En Chimie Inorganique), Université de Reims Champagne-Ardenne
BP 1039, 51687 Reims cedex 2 (France)
Fax: +33-3-26913243
E-mail: emmanuel.guillon@univ-reims.fr

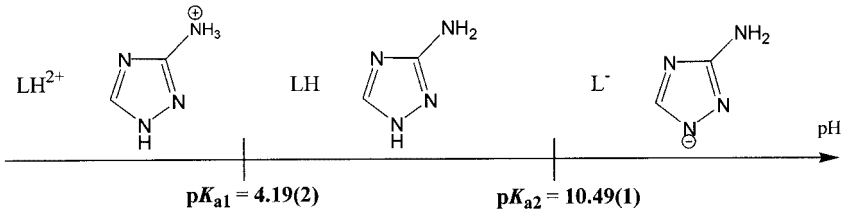

Scheme 1. Different steps of amitrole (LH) deprotonation and their corresponding acidity constants.

tive adsorption data for the three binary systems: aqueous amitrole–Cu^{II}, amitrole–LS and Cu^{II}–LS. We will emphasise how the adsorption characteristics and surface speciation of amitrole are affected by the presence of Cu^{II}, and vice versa. This is the first time that spectroscopic results have been presented for this ternary system, and they allow a good understanding of the molecular mechanism of amitrole retention by SOM in the presence of Cu^{II}.

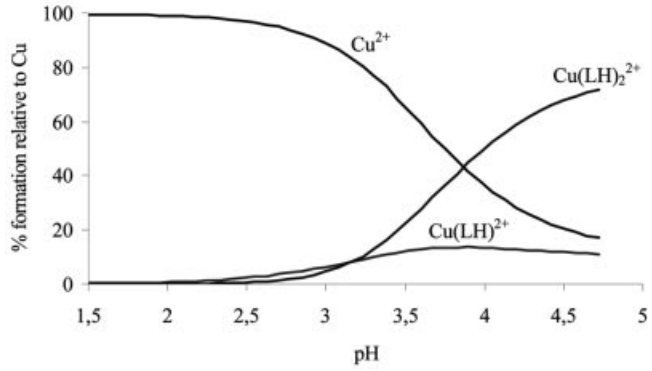

Figure 1. Distribution curves. $C_L = 1.2 \times 10^{-2}$ mol L^{-1}, $C_M = 2.4 \times 10^{-3}$ mol L^{-1}.

Results and Discussion

Binary Systems

The deprotonation reactions of amitrole were studied in KNO_3 (0.1 mol L^{-1}) in the pH range 2–12. The two acidity constants and the deprotonation steps of amitrole are reported in Scheme 1. The constant pK_{a1} corresponds to the deprotonation of the exocyclic nitrogen atom and the constant pK_{a2} to the deprotonation of the endocyclic nitrogen atom. These values are close to the ones obtained by Pichon and Hennion,[16] and Boraei and Mohamed[17] under similar conditions.

The first binary system, Cu^{II}–amitrole, was then studied in aqueous solution by titration with 0.1 mol L^{-1} KOH (ionic strength = 0.1 mol L^{-1}) at variable C_L/C_{Cu} ratios (total ligand to total copper concentration; R). The ligand concentration, C_L, was kept constant (1.2×10^{-2} mol L^{-1}) and the ratio R ranged from 1.08 to 5. The experimental data are shown as distribution curves in Figure 1. It is obvious from this figure that Cu^{II} complexation becomes significant at pH values above 2.5. As formation constant calculations can only be made in a homogeneous medium, the precipitation of a mixed hydroxo-amitrole copper complex since around pH 5 prevents any calculations above this value. Unfortunately, this precipitated complex could not be obtained as a pure compound, but the presence of amitrole was identified by IR spectroscopy. Calculations showed that the best fit between the calculated curves and the experimental data (volume of KOH added, pH) was obtained with two successive complexes having the compositions $Cu(LH)^{2+}$ and $Cu(LH)_2^{2+}$. The logarithmic values of the overall formation constants (log β_n) for these two species are equal to 12.5 and 26.0, respectively. The overall constants $\beta_n = [Cu(LH)_n^{2+}]/[Cu^{2+}][L^-]^n[H^+]^n$ correspond to the general equilibrium $Cu^{2+} + nH^+ + nL^- \rightleftharpoons Cu(LH)_n^{2+}$.

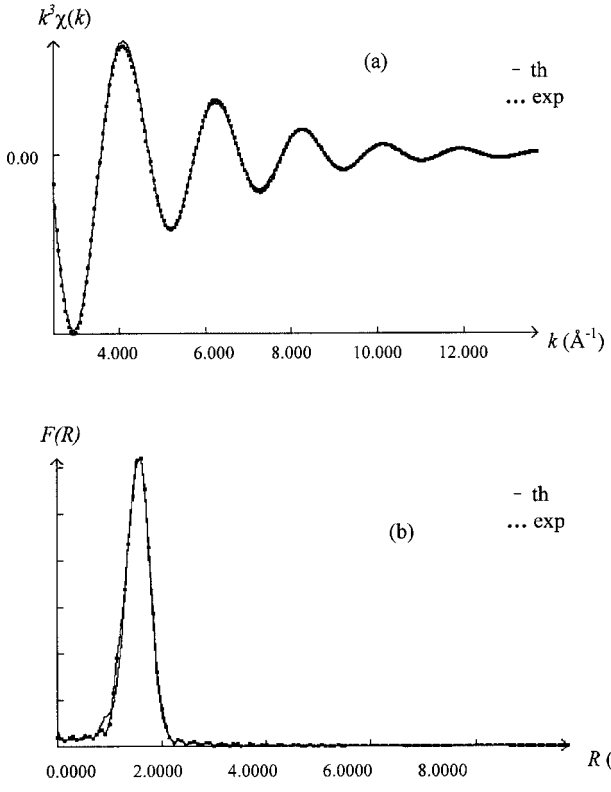

Figure 2. (a) Experimental and fitted first shell (0.96–2.10 Å^{-1}) EXAFS k space spectra of Cu-amitrole solution complex. (b) Fourier transform of the EXAFS signal [$k^3\chi(k)$] at the copper K edge.

The overall stability constants combined with acidity constants lead to the successive complexation constants K_n, which correspond to the equilibrium $Cu^{2+} + n$LH $\rightleftharpoons$ $Cu(LH)_n^{2+}$.

The logarithmic values of the constants K_n are equal to 2.0 (n = 1) and 3.0 (n = 2). The unexpected variation of these constants ($\log K_1 < \log K_2$) is probably due to a geometric change of the complex or to the Jahn–Teller effect.

In order to obtain structural information about the copper–amitrole complex in solution, UV/visible spectroscopy and XAS experiments were carried out. In the visible region, the absorption spectrum exhibits a broad non-symmetric band centred around 15335 cm^{-1} characteristic of a tetragonal elongated octahedral environment around copper(II) with a CuN_2O_4 chromophore.[18] The structure of the complex in solution was also studied by EXAFS spectroscopy. The first shell was best fit with four oxygen/nitrogen atoms (Figure 2) at an average distance of 2.04 Å from the absorbing copper atom. These four atoms are most likely positioned in the equatorial plane of a Jahn–Teller-distorted, elongated octahedron, similar to the arrangement described for $Cu(OH)_2$.[19] The two axial oxygens of the octahedron are more distant from the copper atom and form weaker bonds, giving rise to higher thermal disorder. These atoms are therefore not expected to contribute significantly to the EXAFS signal. Attempts to fit oxygen at axial positions indeed resulted in high Debye–Waller factors for these atoms (>0.015), and there was no improvement in the fit, compared to including only equatorial oxygen/nitrogen atoms. These EXAFS results combined with those obtained by UV/visible spectroscopy clearly show that the copper in the $Cu(LH)_2^{2+}$ complex is surrounded in the equatorial plane by two nitrogen atoms from amitrole and two water oxygen atoms. The axial position is occupied by two other water molecules. This structure is represented in Scheme 2.

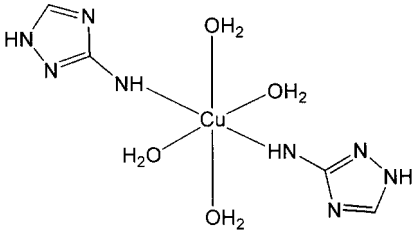

Scheme 2. Molecular structure of $Cu(LH)_2^{2+}$ in solution.

In a second step, we studied the amitrole sorption onto LS as a function of pH. Surprisingly, amitrole was not retained by LS in the pH range 2–12 (Figure 3). This result is unexpected since analogous pesticides are well known to bond to the SOM surface through electrostatic bonds.[20–22] This means that amitrole in a soil with a high content of organic matter such as lignin will be leached towards the surface- and groundwater.

The last binary system is the Cu^{II}–LS system. Copper retention on the solid has been studied previously and the results published in terms of quantitative data[23] and a molecular approach.[24] Briefly, copper is quantitatively sorbed (4.2 mg g^{-1}) at the LS surface. It is surrounded by four oxygen atoms at 1.93 Å and two other ones at 2.41 Å, which corresponds to a tetragonal-distorted octahedral geometry.

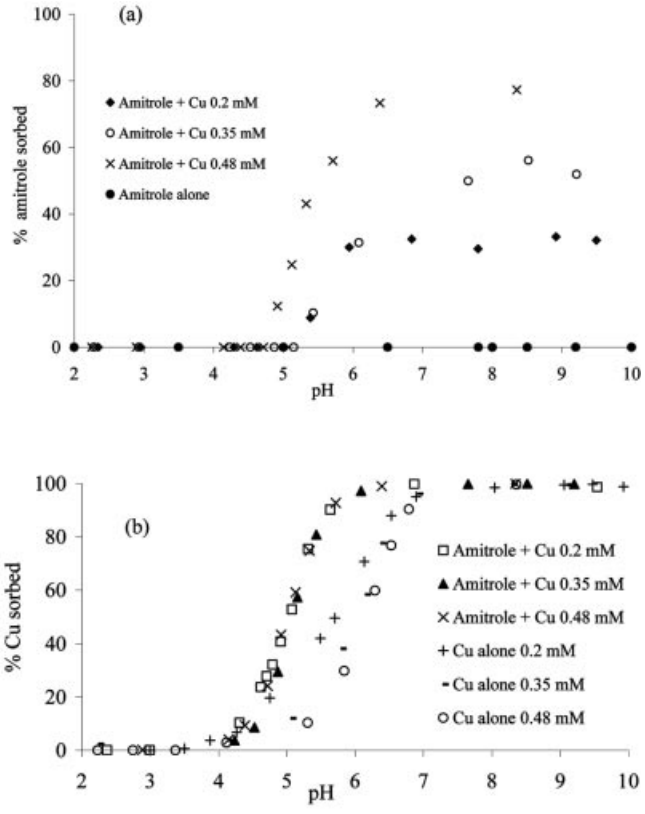

Figure 3. Adsorption of amitrole and Cu^{II} on the LS surface as a function of pH. $C_{amitrole}$ = 0.5 mmol L^{-1}.

Ternary System

The ternary system involving LS, Cu^{II} and amitrole was then studied by means of batch adsorption experiments combined with spectroscopic studies to obtain molecular-level information with the aim of understanding the coadsorption process. Figure 3 shows the adsorption of amitrole, Cu^{II} and both amitrole and Cu^{II} as functions of pH at three different total concentrations of Cu^{II}. The amount of amitrole adsorbed in the presence of Cu^{II} increases proportionally with the introduced copper concentration (Figure 3a). At the same time, all the copper added (three different concentrations) is adsorbed even in the presence of amitrole (Figure 3b). Indeed, in the presence or absence of amitrole, 100% of the copper introduced is sorbed above pH 7. This is in accordance with a mechanism of formation of a ternary complex in two steps: formation of the copper–amitrole complex $Cu(LH)_2^{2+}$ in solution followed by the sorption of this complex onto the LS surface, which leads to the Cu^{II}–amitrole–LS ternary complex, since amitrole alone is not adsorbed onto the LS surface. Moreover, as expected for the three copper concentrations studied, the amount of ligand, copper and copper–amitrole complex adsorbed increases with increasing pH. This enhancement is characteristic of the sorption of a cationic species [$Cu(LH)_2^{2+}$] on a surface, which confirms the mechanism previously proposed for the retention of amitrole in the presence of copper through ternary surface complex formation.

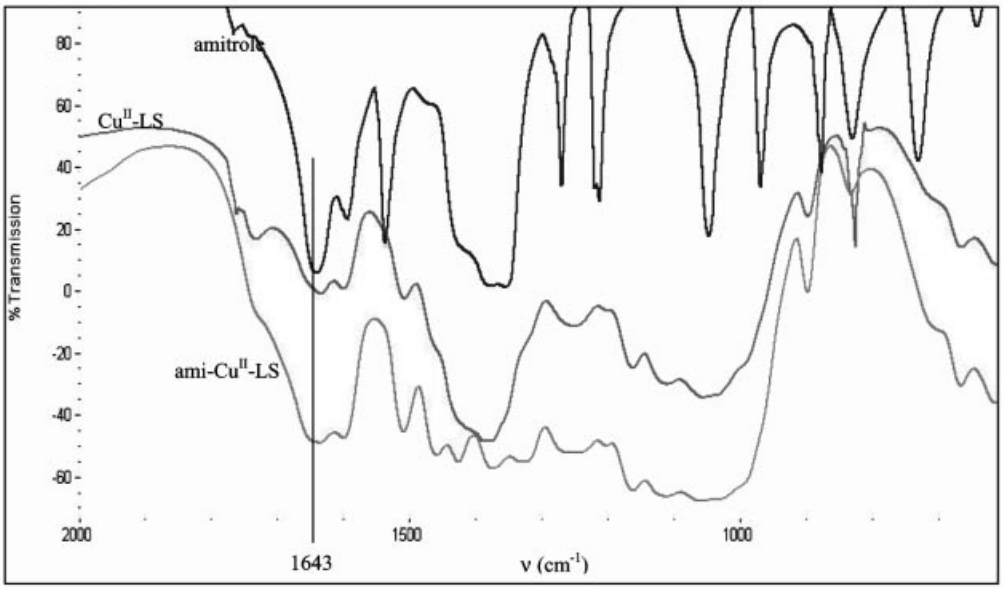

Figure 4. IR spectra of amitrole alone and the Cu^{II}-LS and ami-Cu^{II}-LS systems.

Moreover, the formation of 1:1 [Cu(LH)$^{2+}$] metal/ligand surface complexes cannot be ruled out, since the distribution curves (Figure 1) show the presence of 10% of the Cu(LH)$^{2+}$ species around pH 4–5.

The latter was confirmed by spectroscopic studies, from which structural information were obtained. The IR spectrum of amitrole shows several characteristic absorption bands, in particular the band at 1643 cm^{-1}, which corresponds to the C–N stretching band of the C–NH$_2$ exocyclic group, and the one at 1537 cm^{-1} corresponding to the conjugated ring C=N stretching vibration.[15] The IR spectrum of the Cu^{II}–amitrole–LS sample shows the disappearance of the latter, probably due to the low amitrole concentration on LS. The formation of a ternary complex was confirmed by the presence of a supplementary very weak band characteristic of amitrole at 1643 cm^{-1}, as compared to the Cu^{II}–LS spectra (Figure 4).

XAS experiments were carried out in order to obtain structural information about the ternary surface complex. The *K*-edge XANES spectrum and its first derivative are shown in Figure 5. They are typical of copper(II) complexes with a very weak 1s→3d transition pre-edge feature centred around 8978 eV, which is facilitated by p-d mixing,[25] and an absorption edge centred around 8996 eV. The most important feature of the spectrum at the copper edge is that the low-energy side of the edge exhibits the characteristic shoulder of copper(II) in an elongated tetragonal surrounding.[26] In Figure 5b, in addition to the very weak pre-edge peak, there is a splitting of peaks α and β in the first derivative Cu XANES spectrum. This first derivative can reveal detailed information that is not obvious in this XANES spectrum. The peak α corresponds to the 1s→4p$_{x,y}$ transitions. The second main peak (β) represents the main absorption transition (1s→continuum). The energy gap between the α and β peaks is equal to 6.2 eV. This value gives an estimate of the destabilization of the 4p$_z$ metal orbital (z being the elongation axis). Indeed, it has been suggested that in elongated tetragonal copper(II) complexes, the further the apical site from the metal ion the more displaced this shoulder is towards low energies.[27] The average axial distance around the copper atom was estimated at approximately 2.4 Å by comparison with reference compounds.[24]

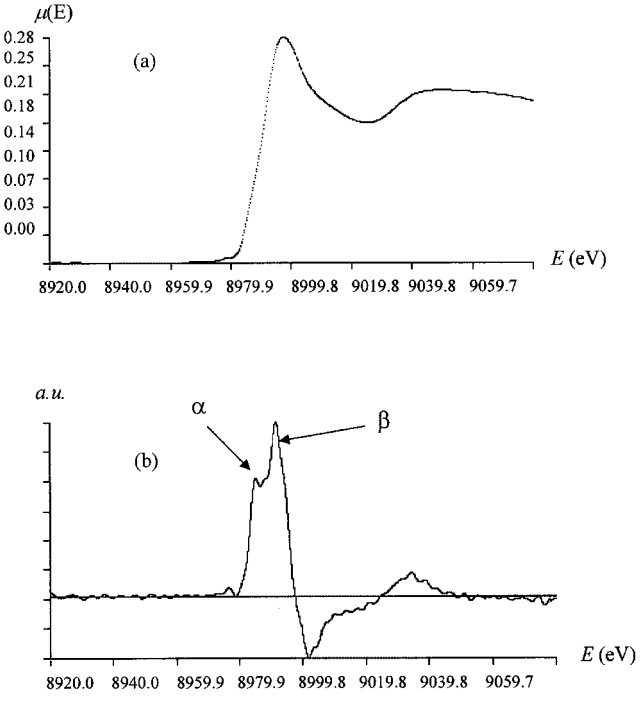

Figure 5. Cu *K*-edge XANES spectrum of the Cu-amitrole-LS ternary complex (a), and its first derivative (b).

The experimental data and the fitted functions of the ternary system first shell are shown in k space as well as by Fourier transformations in real space in Figure 6. In agreement with the previous results, we found four copper–oxygen/nitrogen average distances of 2.01 Å (σ = 0.001 Å^2) from the adsorbing copper atom. Attempts were made to determine also the two longer axial distances, and two Cu–OH_2 distances equal to 2.36 Å (σ = 0.008 Å^2) were found. These data are consistent with those obtained from the XANES spectrum, i.e. a tetragonally distorted octahedral coordination around copper(II), according to the Jahn–Teller effect. The weak scattering contribution from low-Z elements beyond the first shell to the EXAFS, seen as minor Fourier peaks, prevents a more detailed analysis. However, a structure for the ternary surface complex can be proposed (Scheme 3). In Figure 7, for comparison, the k^3-weighted EXAFS spectra and Fourier transforms are reported for Cu^{II} adsorbed together with amitrole on LS, the $Cu(LH)_2^{2+}$ aqueous complex, and Cu^{II} adsorbed onto LS. Even the EXAFS spectra seem identical, although a faint difference can be observed on the first beating of the sinusoid around 4 Å^{-1}, which is also observed for the Cu^{II}–O/N distances. Indeed, the Cu–O/N distance in the Cu-LS surface complex is equal to 1.93 Å,[24] that in the $Cu(LH)_2^{2+}$ aqueous complex to 2.04 Å, and that in the ternary complex to 2.01 Å. The intermediate value obtained for the ternary complex leads to the proposed structure in which two copper–amitrole and two copper–LS bonds are in the equatorial plan, and two water molecules are in the axial positions. This also rules out a surface precipitation of a mixed hydroxo-amitrole copper complex (see solution chemical study). Moreover, the Fourier transform of the ternary surface complex corresponds to the weighted sum of the Fourier transforms of $Cu(LH)_2^{2+}$ and Cu-LS complexes (Figure 7).

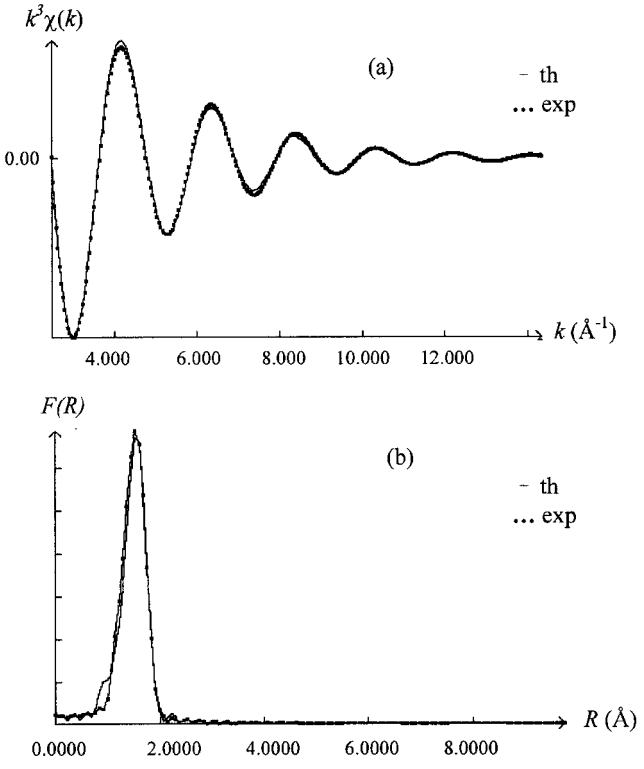

Figure 6. (a) Experimental and fitted first shell (1.16–2.02 Å^{-1}) EXAFS k space spectra of the Cu-amitrole-LS ternary complex. (b) Fourier transform of the EXAFS signal [$k^3\chi(k)$] at the copper K edge.

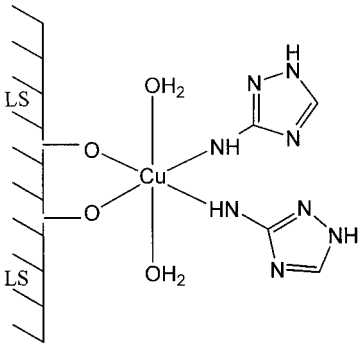

Scheme 3. Proposed structure of the ternary Cu^{II}–amitrole–LS surface complex.

Conclusions

By simultaneously using quantitative and spectroscopic methods we have shown that Cu^{II} and amitrole form ternary complexes on soil organic matter. The retention of amitrole is only possible in the presence of copper. A lack of copper leads to the leaching of the pesticide to surface- and/or groundwater. Potentiometric titrations have underlined the existence of a predominating complex, $Cu(LH)_2$, which was confirmed by IR spectroscopy. Adsorption isotherms and XAS data indicate a molecular structure where copper(II) bonds to the surface in an inner-sphere mode. According to solution studies combined with adsorption and XAS experiments, we have proposed a possible structure for the ternary complex. Two amitrole ligands are probably monodentately bound to Cu^{II} and the copper coordination sphere is completed by two water molecules to form a six-membered coordination sphere around the metal cation (Scheme 3). Finally, it is now obvious that metal ions have a significant influence on the molecular surface speciation of amitrole. The new structure identified is potentially important for elucidating the bio-availability and mechanisms of amitrole degradation in soils. The results obtained in this study are currently being used with modelling software to establish predictive systems for the retention of pesticides in soils in the presence of metallic cations.

Experimental Section

Reagents: All solvents and chemicals from commercial sources were of the highest available purity and were used without further purification. The metal-ion stock solutions were prepared from copper(II) nitrate reagents (Fluka) of the highest purity (>99%). The concentration was determined by EDTA titration {with PAN [1-(2-pyridyl-azo)-2-naphthol] as indicator}. The LS was extracted from

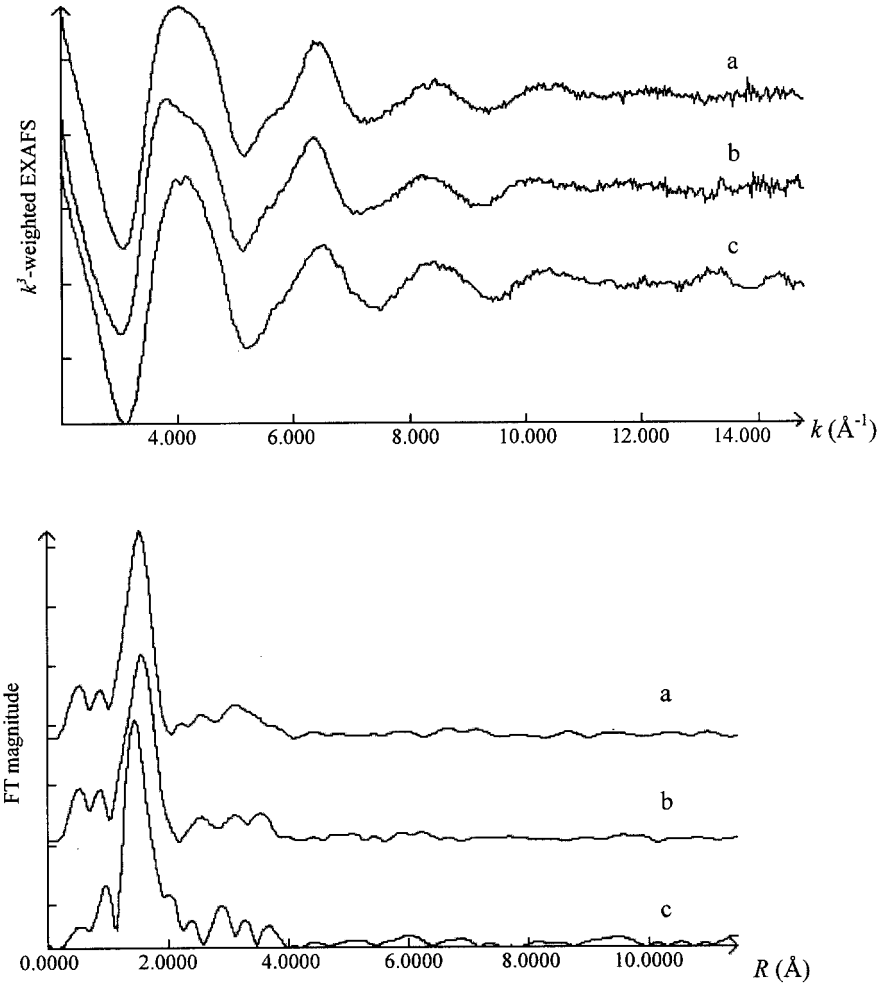

Figure 7. k^3-Weighted EXAFS spectra and Fourier transforms for Cu^{II} adsorbed together with amitrole on LS (a). Included for comparison: k^3-weighted EXAFS spectra and Fourier transforms of (b) $Cu(LH)_2$ (aq.) and (c) Cu^{II} adsorbed on LS.

wheat straw by two successive acid-base treatments,[24] and was fully characterized.[28]

Protometric: Potentiometric titrations were carried out as described previously.[29] Briefly, they were performed with a Metrohm 665 Dosimat and a Metrohm 654 pH-meter. The combined glass electrode was standardized with nitric acid (10^{-2} mol L^{-1}; pH 2.00). All measurements were performed at 20 °C under a nitrogen stream. The curves obtained were fitted with the refining program PROTAF[30] in order to obtain the overall stability constants. The ionic product of water, pK_w, was determined to be 13.78. The concentration of copper(II) varied from 1.09×10^{-2} to 0.24×10^{-2} mol L^{-1}, the concentration of the ligand from 8×10^{-3} to 2×10^{-2} mol L^{-1} and the ratio C_L/C_M from 1.08 to 5. The ionic strength was kept constant (0.1 mol L^{-1}) by addition of potassium nitrate.

Sorption Experiments: Adsorption experiments were conducted as a function of pH using batch experiments at room temperature (293 K). The LS (2 g L^{-1}) was immersed in 15 mL of background electrolyte (0.1 mol L^{-1} KNO_3) solution and stirred with a magnetic stir bar for 24 h, which corresponds to the hydration time of the solid. After this pre-equilibration step, the amitrole (5×10^{-4} mol L^{-1}) was added simultaneously with copper (2×10^{-4}, 3.5×10^{-4} and 4.8×10^{-4} mol L^{-1}), and the pH was incrementally adjusted to a fixed value by dropwise addition of 0.1 mol L^{-1} HNO_3 or 0.1 mol L^{-1} KOH. The final volume was adjusted to 25 mL. The sorption equilibrium (12 h) was predetermined by kinetic experiments in which different contact times from 10 min to 48 h between the sorbents and the solid were applied. When two successive curves were superimposed, the equilibrium time was considered to have been reached. The flasks were then shaken at 293 K for 12 h with an automatic shaker to ensure complete sorption. The experimental pH was taken to be the pH measured after a 12 h reaction time. After filtration through a 0.20 μm polyamide membrane, the supernatants were separated into two fractions. In the first fraction, the solution was acidified and the unsorbed metal-ion concentration was measured with a Varian ICP-AES spectrometer. The amount of copper sorbed was deduced from the initial concentration. The amount of amitrole was determined from the second fraction using the spectrophotometric method described by Sund.[10]

The solid studied by spectroscopic techniques was prepared at pH 5.7 with a copper concentration equal to 2×10^{-4} mol L^{-1} and an amitrole concentration of 5×10^{-4} mol L^{-1}. This pH value was chosen in order to have a maximum copper amount adsorbed and to prevent copper hydroxide precipitation (pH 6.8).

Spectroscopy: The electronic spectra in aqueous solutions were recorded in a 1.00-cm quartz cell with a Perkin–Elmer Lamba-6 UV/Visible spectrophotometer. IR spectra were obtained in pellets with a Nicolet Avatar 320 spectrophotometer.

EXAFS and XANES Data: The XAS experiments were performed on the XAS 4 beamline of the storage ring DCI (positron energy 1.85 GeV; mean current 300 mA) at LURE (Laboratoire d'Utilisation du Rayonnement Electromagnétique, Paris-Sud University). Data were recorded at the Cu *K* edge (8979 eV) using a channel-cut monochromator Si(111) for EXAFS and Si(311) for XANES. The solids and the aqueous copper(II) solutions were measured at room temperature in the transmission mode with two air-filled ionisation chambers. Internal calibration was made with a copper metal foil and fixed at 8979 eV for the first inflection point. Four scans were summed for the samples. The XANES spectra were recorded step-by-step, every 0.3 eV, with a 2 s accumulation time per point. The spectrum of the 5 μm metallic foil was recorded just before the unknown XANES spectrum to check the energy calibration, thus ensuring an energy accuracy of 0.25 eV. The EXAFS spectra were recorded over 1000 eV, with 2 eV steps, from 8900 to 9900 eV. Data analysis was performed by means of the "EXAFS pour le Mac" package.[31] The $\chi(k)$ functions were extracted from the data with a linear pre-edge background, a combination of polynomials and spline atomic-absorption background, and normalised using the Lengeler–Eisenberg method.[32] The energy threshold, E_0, was taken at the middle of the absorption edge and was corrected for each spectrum in the fitting procedure. The k^3 weighted $\chi(k)$ function was Fourier transformed from k = 2–14 Å^{-1}, by means of a Kaiser–Bessel window with a smoothness parameter equal to 3 (k is the photoelectron wave number). In this work, all Fourier transforms were calculated and presented without phase correction. The peaks corresponding to the first coordination shell were then isolated and back-Fourier transformed into k space to determine the mean coordination number, N, the bond length, R, and the Debye–Waller factor, σ. The resulting EXAFS functions were curve-fitted by calculated model functions using ab initio calculated EXAFS phase $|\varphi_i(k,R_i)|$ and amplitude $|f_i(k,R_i)|$ parameters from FEFF7 code.[33] The errors in the first shell bond lengths (R) were estimated to be ±0.02 Å and coordination numbers (N) were accurate to ±20%.

Acknowledgments

We are grateful to the "Région Champagne-Ardenne" for a grant to K.F. The authors also wish to acknowledge S. Belin (Université Paris Sud, LURE, France) for her help in recording EXAFS and XANES data.

[1] A. Manceau, M. L. Schlegel, M. Musso, V. A. Sole, C. Gauthier, P. E. Petit, F. Trolard, *Geochim. Cosmochim. Acta* **2000**, *64*, 3643–3661.
[2] L. Charlet, A. Manceau, *J. Colloid Interface Sci.* **1992**, *148*, 443–458.
[3] S. E. Fendorf, G. M. Lamble, M. G. Stapleton, M. J. Kelley, D. L. Sparks, *Environ. Sci. Technol.* **1994**, *28*, 284–289.
[4] J. C. Echeverria, M. T. Morera, C. Mazkiaran, J. J. Garrido, *Environ. Pollut.* **1998**, *101*, 275–284.
[5] S. E. Bailey, T. J. Olin, R. M. Bricka, D. D. Adrian, *Water Res.* **1999**, *33*, 2469–2479.
[6] A. Kokorevics, J. Gravitis, E. Chirkova, O. Bikovens, N. Druz, *Cell. Chem. Technol.* **1999**, *33*, 251–266.
[7] P. Merdy, E. Guillon, M. Aplincourt, *New J. Chem.* **2002**, *26*, 1638–1645.
[8] E. Ammälahti, G. Brunow, M. Bordet, D. Robert, I. Kilpeläinen, *J. Agric. Food Chem.* **1998**, *46*, 5113–5117.
[9] R. T. Meister, in *Chemicals Handbook '92* (Meister Publishing Company), Willoughby, OH, USA, **1992**.
[10] K. A. Sund, *J. Agric. Food Chem.* **1956**, *4*, 57–60.
[11] C. D. Ercegovich, D. E. H. Frear, *J. Agric. Food Chem.* **1964**, *12*, 26–29.
[12] J. D. Russell, M. I. Cruz, J. L. White, *J. Agric. Food Chem.* **1968**, *16*, 21–24.
[13] D. C. Nearpass, *Soil Sci.* **1970**, *109*, 77–84.
[14] T. Oesterreich, U. Klaus, M. Volk, B. Neidhart, M. Spiteller, *Chemosphere* **1999**, *38*, 379–392.
[15] E. Morillo, J. L. Pérez-Rodriguez, C. Maqueda, *Clays Clay Miner.* **1991**, *26*, 269–279.
[16] V. Pichon, M. C. Hennion, *Anal. Chim. Acta* **1993**, *284*, 317–326.
[17] A. Boraei, M. C. Mohamed, *Chem. Eng. Data* **2002**, *47*, 987–991.
[18] A. B. P. Lever, in *Inorganic Electronic Spectroscopy*, 2nd ed., Elsevier, Amsterdam, **1984**.
[19] M. Magini, *J. Chem. Phys.* **1981**, *74*, 2523–2529.
[20] N. Senesi, *Sci. Total Environ.* **1992**, *123–124*, 63–76.
[21] M. J. Salloum, B. Chefetz, P. G. Hatcher, *Environ. Sci. Technol.* **2002**, *36*, 1953–1958.
[22] H. R. Schulten, B. Plage, M. Schnitzer, *Naturwissenschaften* **1991**, *78*, 311–312.
[23] P. Merdy, E. Guillon, M. Aplincourt, J. Dumonceau, H. Vezin, *J. Colloid Interface Sci.* **2002**, *245*, 24–31.
[24] E. Guillon, P. Merdy, M. Aplincourt, *Chem. Eur. J.* **2003**, *9*, 4479–4484.
[25] J. E. Hahn, R. A. Scott, K. O. Hodgson, S. Doniach, S. Desjardins, E. I. Solomon, *Chem. Phys. Lett.* **1982**, *88*, 595–598.
[26] N. Kosugi, T. Yokoyama, K. Asakuna, H. Kuroda, *Chem. Phys.* **1984**, *91*, 249–256.
[27] C. Surville-Barland, R. Ruiz, A. Aukauloo, Y. Journaux, I. Castro, B. Cervera, M. Julve, F. Llord, F. Sapina, *Inorg. Chim. Acta* **1998**, *278*, 159–169.
[28] P. Merdy, E. Guillon, J. Dumonceau, M. Aplincourt, *Anal. Chim. Acta* **2002**, *459*, 133–142.
[29] E. Guillon, P. Merdy, M. Aplincourt, J. Dumonceau, H. Vezin, *J. Colloid Interface Sci.* **2001**, *239*, 39–48.
[30] R. Fournaise, C. Petitfaux, *Talanta* **1987**, *34*, 385–395.
[31] A. Michalowicz, EXAFS pour le Mac, Logiciel pour la Chimie, Société Française de Chimie, Paris **1991**, p. 102.
[32] B. Lengeler, P. Eisenberg, *Phys. Rev. B* **1980**, *21*, 4507–4518.
[33] S. I. Zabinsky, J. J. Rehr, A. Ankudinov, R. C. Albers, M. J. Eller, *Phys. Rev. B.* **1995**, *52*, 2995–3009.

Received: September 14, 2004

